



Numerical study of meso-scale circulation specifics in the Sofia region under different large-scale conditions

Evgenia Egova^{1,2*}, Reneta Dimitrova¹, Ventsislav Danchevski¹

¹*Faculty of Physics, Department of Meteorology and Geophysics - Sofia University "St. Kliment Ohridski", 5 James Bourchier Blvd., 1164 Sofia, Bulgaria*

²*National Institute of Meteorology and Hydrology - BAS, 66 Tsarigradsko shose Blvd., 1784 Sofia, Bulgaria*

Abstract: Accurate airflow forecast over large urban areas in complex orography is very important problem and it is still a big challenge. Terrain and land-cover inhomogeneity cause thermal circulation domination under calm conditions, or significant modification of the large-scale synoptic flow. The Weather Research and Forecasting (WRF) model is used for numerical experiments with fine horizontal grid of 500 meters. The static terrestrial data are represented with very high resolution (1 arcsec for the orography and 3 arcsec for land-cover data). The purpose of this work is to assess the ability of WRF model to study the specifics of meso-scale circulation under various large-scale (synoptic) conditions for the Sofia region. Different model options (for microphysics and planetary boundary layer - PBL) are tested during the evaluation process based on comparison to measurements in order to determine the optimal configuration. Overall Lin et al. microphysics scheme shows the best performance. None of the PBL schemes is found to be superior, but all provide reasonable results. WRF model shows good performance and it is a very useful tool to study flow structure and variability. Different mesoscale phenomena are properly captured with numerical simulations.

Keywords: flow modification over complex orography, meso-scale phenomena, WRF, model sensitivity tests, evaluation for Sofia region.

1. INTRODUCTION

Several types of investigation (theory, numerical modelling and laboratory experiments) are used to study atmospheric dynamics and physics that play an important role in atmospheric processes. The analytical theory is limited to simplified equations

* evgenia.egova@abv.bg

that are unable to describe fully the atmosphere in its complexity. The advantages of laboratory experiments are their simplicity and directness, but not all major phenomena can be simulated (Tucker, 1989; Baines&Manins, 1988). Numerical modeling is a main tool for studying the phenomena in atmosphere and its potential is almost unlimited with fast improvement of computer resources during the last decade.

Meso-scale systems can be defined as those atmospheric systems that have a horizontal extent large enough for the hydrostatic approximation to the vertical pressure distribution to be valid, but small enough for the geostrophic and gradient winds to be inappropriate as approximations to the actual wind circulation above the planetary boundary layer (Pielke, 2013). Many different classifications are used in the literature. One of the most popular classifications (Orlanski, I., 1975) divides meso-scale systems into 3 sub-categories with horizontal scales for meso-gama between 2 and 20 km; meso-beta 20-200 km; and meso-alpha 200-2000 km. Some of the processes in the meso-alpha are at the edge of the synoptic systems which horizontal scales can start from 1000 km. This study investigates the atmospheric phenomena in meso-gama scale. Terrain and land-use inhomogeneity cause local thermally driven wind systems dominant under calm conditions (Zardi and Whiteman, 2012), or significant modification of the synoptic flow (Bretherton et al., 2009; Dixit&Chen, 2011).

Orography presents significant forcing on geophysical flows and induce substantial adjustment of the large-scale flow. The strong airflow under stratified conditions generates lee waves, propagating internal waves, rotors, flow separation or canalization and fascinating vortex structures. The part of the flow above the so-called dividing streamline goes over the mountain whilst the rest flows around the mountain (Snyder et al., 1985) producing upstream stagnation, the lee-side separation region and associated wake effects. The inhomogeneity of the flow, irregular protrusions from an obstacle in the direction of the approaching flow, slope angle, ground roughness lead to very complicated pattern. The varieties that incorporate slopes, valleys, canyons, escarpments, gorges and bluffs span different space-time scales contributing to innumerable phenomena that stymie the predictability of mountain weather.

Diurnal mountain winds develop typically under fair weather conditions, over complex topography of all scales, from small hills to large mountain massifs, and are characterized by a reversal of wind direction twice per day (Zardi&Whiteman, 2012). In the surface heated planetary boundary layer (PBL) landscape heterogeneities produce significant horizontal gradients in temperature that form phenomena like land and sea breezes. All these local thermally driven meso-scale circulations can be accelerated or suppressed by the large-scale flow. Urbanization in the post-industrial revolution era, especially the recent rapid urban growth, has brought about unprecedented anthropogenic stressors that may change the functioning and structure of the Earth system or a part thereof (Hunt et al., 2007). Intense modification of land surface occurs through urban development (Changnon, 1992), and the use of high heat capacity and water impermeable material for construction and roadways affects local microclimates. The differences in

energy balance, temperature, humidity, and storm runoff between urban areas and rural surfaces are substantial. A common urban effect is the urban heat island associated with the retention of heat in concrete and other material for longer times at night in urban compared to rural areas (Bornstein, 1987; Oke, 1988; Emmanuel&Fernando, 2007).

Sofia city is located in complex terrain in close proximity to Vitosha Mountain with highest peak Cherni vrah – 2286 m AGL (above ground level). All described factors above contribute to a very complicated flow pattern in Sofia valley that is difficult to predict. The purpose of this work is to investigate the abilities of the Weather Research and Forecasting (WRF) model to capture the specifics of the meso-scale circulation under different large-scale conditions for the Sofia region. Very high resolution static terrestrial fields (1 arcsec for the topography and 3 arcsec for land cover) are used in this study. Performance evaluation of different parameterization schemes (for both microphysics and PBL) is accomplished through comparison with observation.

2. DATA AND METHODOLOGY

The Advanced Research version of the Weather Research and Forecasting model (ARW-WRFv3.8.1.) is employed in this study. The ARW-WRF is a state-of-the art atmospheric meso-scale numerical weather prediction system, suitable for use in a broad range of applications (Skamarock et al., 2008; <http://www.mmm.ucar.edu/wrf/users>). The system solves fully compressible, Euler non-hydrostatic equations conservative for scalar variables, over terrain-following vertical coordinates with the possibility of vertical grid stretching. The upper boundary of the model is a constant pressure surface.

2.1. Domain set-up and initial conditions

A Lambert Projection is used with the center point for the modelling domain at 23.4°E, 42.68°N. Four nested domains with 32, 8, 2 and 0.5 km grid resolution are explored to perform meso-scale simulations, with the smallest one covers the Sofia valley. The model domains with an enlarged view of the most inner domain with 500 m resolution and 157x129 grid points (approximately 80x65 km) is shown Fig. 1.

Fifty terrain-following (η) levels are selected, with 21 levels between the surface and 500 m AGL to describe better the lowest part of the PBL. Meteorological initial and boundary conditions are provided to the coarsest meso-scale simulations from the National Centers for Environmental Prediction (NCEP) Final Analysis 0.25 degrees with outputs every 6 h (<http://rda.ucar.edu/datasets/ds083.2/>). Two new datasets have been implemented and adapted to the study domain - high resolution topography data (SRTM, NASA; <https://lta.cr.usgs.gov/SRTM1Arc>) with resolution 1 arcsec (approximately 30 m), and the Corine land-cover dataset (CLC2012, EEA; <http://land.copernicus.eu/pan-european/corine-land-cover/clc-2012>), with resolution 3 arcsec (approximately 90 m), which have been adopted to US Geological Survey land-use (USGS) classes.

More details regarding the procedure and new datasets implementation can be found in Vladimirov et al. (2018).

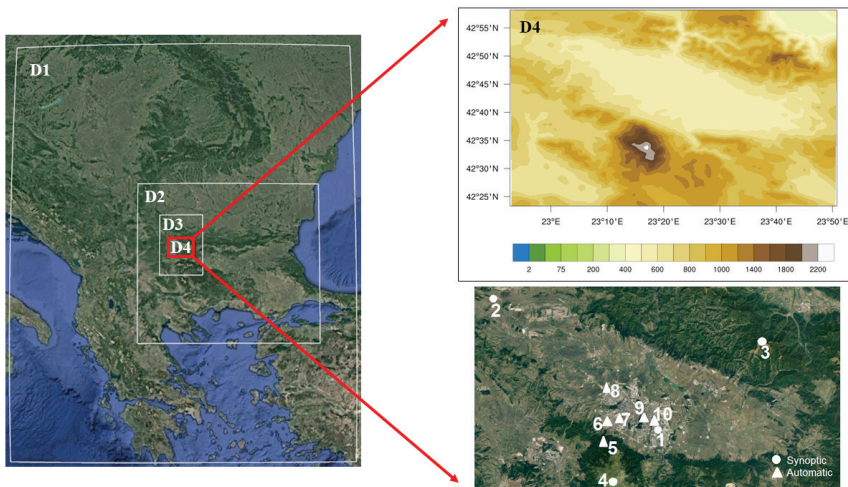


Fig. 1. Domain configuration (left panel); topography of the most inner domain (500 m grid) and location of the observational sites used for model validation (right panel).). SYNOP stations (circle symbol): 1. Sofia, 2. Dragoman, 3. Murgash, 4. Cherni vrah and Automatic stations (triangle symbol): 5. Kopitoto 6. Pavlovo 7. Hipodruma 8. Nadezhda 9. Borisova gradina and 10. Druzhba

2.2 Model options

The WRF physics package includes: the Rapid Radiative Transfer Model (RRTM) longwave radiation parameterization (Mlawer et al., 1997), Dudhia shortwave radiation parameterization (Dudhia, 1989), which computes radiation at fine time scales (every 10 min), and Grell-Devenyi (GD) ensemble scheme (Grell&Devenyi, 2002) for cumulus parameterization (only for the coarse meso-scale simulation with 32 and 8 km grids). Noah land surface model scheme (Chen&Dudhia, 2001) is chosen for this study. Four of the available in the model PBL schemes (with their corresponding surface schemes) are considered after preliminary comparison against observations in previous studies. The selected PBL schemes are: the Yonsei University scheme, YSU (Hong et al., 2006), the Asymmetric Convective Model, version 2 scheme, ACM2 (Pleim, 2007), the Bougeault and Lacarrere scheme, BouLac (Bougeault&Lacarrere, 1989), and the Quasi-Normal Scale Elimination scheme, QNSE (Sukoriansky et al., 2005). In addition comparison between model results for different microphysics schemes are conducted for one case with very high humidity (February 5th 2016). The YSU PBL scheme is used with four available microphysics options, all of them suitable for real-data high-resolution

simulations: a sophisticated scheme Lin et al. (Lin et al., 1983), WRF Single-Moment 6 (Hong&Lim, 2006), Goddard (Tao et al., 1989) and Thompson (Thompson et al., 2008).

2.3. Case studies selection

This study exemplifies the ability of WRF model to represent properly the meso-scale circulation in Sofia valley and study flow modification under different synoptic conditions. Nine cases between summer 2015 and summer 2016 are selected using weather maps for flow and temperature at 850 hPa and observational data from the radiosonding made once a day at 12 UTC at the National Institute of Meteorology and Hydrology (NIMH), Bulgarian Academy of Sciences (BAS). Sofia valley's orientation is Northwest-Southeast and flow directions along the axis (Northwest (NW) and Southeast (SE)) and across (Southwest (SW) and Northeast (NE)) are chosen for the simulations. The case studies are described in Table 1 - calm conditions (wind speed is lower than 5 m/s) and two classes depending on the wind speed – moderate (between 5 and 10 m/s) and strong (wind speed is higher than 10 m/s). Most of the cases, presented in Table 1, are associated with passage of atmospheric disturbance (cyclone or trough) over the Balkan Peninsula and with significant change in 850 hPa temperature. Due to the dynamics of the processes wind conditions are relatively fast changing. All simulations are run with spin-up of 24 hours before each of the selected cases.

Table 1. 9 cases (10 days) of simulations between August 2015 and August 2016.

Cases	Start (UTC)	End (UTC)	Wind Description	Wind Speed
Case 1	14/08/2016 00:00	16/08/2016 00:00	Calm	< 5 m/s
Case 2	04/01/2016 00:00	05/01/2016 00:00	Moderate SW	5 – 10 m/s
Case 3	06/08/2015 00:00	07/08/2015 00:00	Moderate NE	5 – 10 m/s
Case 4	11/11/2015 00:00	12/11/2015 00:00	Moderate NW	5 – 10 m/s
Case 5	22/10/2015 00:00	23/10/2015 00:00	Moderate SE	5 – 10 m/s
Case 6	22/11/2015 00:00	23/11/2015 00:00	Strong SW	> 10 m/s
Case 7	05/02/2016 00:00	06/02/2016 00:00	Strong NE	> 10 m/s
Case 8	25/05/2016 00:00	26/05/2016 00:00	Strong NW	> 10 m/s
Case 9	27/11/2015 00:00	28/11/2015 00:00	Strong SE	> 10 m/s

2.4. Observations

The observational data used for the model validation and sensitivity tests are based on data from ten surface stations, and vertical profiles from radiosonde at one site, National Institute of Meteorology and Hydrology (NIMH), once per day at 12 UTC. The surface stations are: four operational sites (SYNOP) in which data are recorded

every 3 hours: Sofia - NIMH (552 m AGL), Cherni Vrah (2286 m AGL), Murgash (1687 m AGL) and Dragoman (716 m AGL); five automatic stations operated by the Ministry of Environment and Water - Kopitoto (1321 m AGL), Sofia - Nadezhda (534 m AGL), Sofia - Pavlovo (615 m AGL), Sofia -Krasno selo (581 m AGL) and Sofia -Druzhba (548 m AGL), and additional automatic station operated by the Sofia University at Borisova Gradina (577 m AGL) provide hourly records of atmospheric parameters . Air temperatures and relative humidity from all stations are used in model validation. Simulated wind speed and direction are only verified against radiosonde data as all other wind measurements are strongly influenced by obstacles in station's surroundings. The location of observational sites used for model verification are presented in Fig. 1.

3. RESULTS AND DISCUSSION

3.1. Model validation

The model performance at surface level is assessed by comparison of modelled 2m temperature and relative humidity against measurements. Certain statistical accuracy metrics as standard deviation (*SD*), mean bias (*MB*), mean absolute error (*MAE*), root mean square error (*RMSE*), and correlation coefficient (*R*) are also estimated.

Two experiments have been conducted to find the best model configuration by varying PBL and microphysics parameterization schemes at fixed other options. Four different microphysics schemes are tested with the most widely used PBL scheme YSU for one case (Case 7, Table 1) with very high humidity. The selected microphysics option is used further to compare different PBL schemes for all considering cases.

The first experiment considers only Case 7 of Northeastern synoptic flow with high relative humidity (February 5th 2016). For all other selected cases the moisture level is low, relative humidity less than 50%, and the effect of the microphysics option can be ignored. Statistical metrics for two stations are presented - Sofia-NIMH (Table 2) and Borisova gradina (Table 3). The model performs well for both sites, with similar values for different statistical measures. WRF slightly overestimates the temperature with MB, MAE and RMSE values approximately 1°C. The relative humidity is underestimated with about 10% by all considering schemes. The RMSE is higher for the station Borisova gradina with maximum value 17%, than for Sofia-NIMH - 12%. The correlation coefficient is reasonable for all selected microphysics schemes, more than 0.6, as the temperature is better captured at Borisova gradina, the relative humidity at Sofia-NIMH. Overall the Lin scheme shows the best performance for both temperature and relative humidity and it has been selected to be used for the second experiment.

Table 2. Model microphysics evaluation metrics for air temperature and relative humidity in very humid Case 7 (February 5th 2016) at station Sofia-NIMH (number of measurements - 8).

Sofia-NIMH	<i>Mean</i>	<i>SD</i>	<i>MB</i>	<i>MAE</i>	<i>RMSE</i>	<i>R</i>
Temperature [°C]						
Observations	0.0	0.9				
Lin scheme	0.7	0.7	0.7	0.7	0.9	0.75
WRF Single moment 6 class scheme	0.7	0.6	0.7	0.7	1.0	0.65
Goddard scheme	0.5	0.6	0.5	0.5	0.8	0.63
Thompson scheme	0.8	0.6	0.7	0.8	1.0	0.60
Relative Humidity [%]						
Observations	89.6	5.5				
Lin scheme	77.9	6.9	-11.7	11.7	11.9	0.97
WRF Single moment 6 class scheme	79.9	7.9	-9.7	9.7	10.5	0.87
Goddard scheme	81.8	8.7	-7.8	7.8	9.0	0.90
Thompson scheme	78.9	10.1	-10.6	10.8	12.1	0.89

Table 3. Model microphysics evaluation metrics for air temperature and relative humidity in Case 7 (February 5th 2016) at station Borisova gradina (number of measurements - 24)

Borisova gradina	<i>Mean</i>	<i>SD</i>	<i>MB</i>	<i>MAE</i>	<i>RMSE</i>	<i>R</i>
Temperature [°C]						
Observations	-0.3	0.7				
Lin scheme	0.7	0.9	1.0	1.0	1.1	0.86
WRF Single moment 6 class scheme	0.9	0.7	1.1	1.1	1.2	0.69
Goddard scheme	0.5	0.8	0.8	0.8	0.9	0.84
Thompson scheme	0.6	0.8	0.9	0.9	1.0	0.81
Relative Humidity [%]						
Observations	93.5	0.6				
Lin scheme	78.7	8.1	-14.8	14.8	16.7	0.77
WRF Single moment 6 class scheme	79.3	9.8	-14.2	14.3	17.0	0.70
Goddard scheme	82.8	9.3	-10.7	11.0	13.9	0.82
Thompson scheme	82.1	8.7	-11.4	11.5	14.1	0.71

Four different PBL schemes are tested further for all selected study cases described in Table 1. Results of the calculated statistics are presented separately for automatic stations (Tables 4, 5) and SYNOP stations (Table 6). The reason for this separation is that the hourly data from the automatic stations represent more precisely diurnal cycle than data taken on every 3 hours. There is no substantial difference between performances

of the selected PBL schemes. WRF is in better agreement with observations for the cases with moderate (Table 4) than strong (Table 5) wind conditions. The tendency of overestimation of the temperature at 2 m with approximately 1-2°C (mean, *MB*, *MAE*, *RMSE*) is found in all PBL schemes for all study cases. The relative humidity is underestimated with approximately 7% for the moderate (Table 4) and 10% for strong (Table 5) wind conditions. The correlation coefficient differs between schemes and sometimes one scheme performs better for the temperature but worse for the humidity.

Table 4. Model PBL scheme evaluation metrics for air temperature and relative humidity, in cases with moderate wind (Cases 2, 3, 4 and 5) at Borisova gradina, Nadezhda, Pavlovo, Druzhba and Krasno selo (number of measurements - 480).

	<i>Mean</i>	<i>SD</i>	<i>MB</i>	<i>MAE</i>	<i>RMSE</i>	<i>R</i>
Temperature [°C]						
Observations	9.2	2.3				
QNSE	9.9	2.9	0.2	2.1	2.4	0.82
YSU	10.5	2.4	0.7	1.5	1.8	0.82
BouLac	12.9	2.5	1.1	1.9	2.2	0.76
ACM2	10.5	2.7	0.7	1.9	2.1	0.82
Relative Humidity [%]						
Observations	71.4	8.1				
QNSE	72.5	10.1	-1.2	7.9	9.5	0.71
YSU	70.2	8.4	-4.3	7.2	8.2	0.83
BouLac	67.4	8.1	-5.2	7.2	8.3	0.86
ACM2	70.9	8.7	-3.6	7.1	8.3	0.78

The summary of the surface statistics for two SYNOP stations – Sofia and Dragoman (Table 6) shows similar agreement with observations for temperature but worse correlation (less than 0.7) for the relative humidity in comparison with the automatic stations. The errors (*MAE*, *RMSE*) are in the same range – less than 2°C for the temperature and 11% for the relative humidity.

Vertical profiles of modeled atmospheric parameters at NIMH site are compared with derived ones from radiosonde in Fig.2. As an agreement indicator the coefficient of determination (R^2) is also shown. The radiosonde observations (at 12 UTC for all study cases) are interpolated to the model levels at corresponding time. All of the PBL schemes represent well temperature, u and v velocity components, and worse the wind speed and mixing ratio. The best correlation between observations and model data is observed for the temperature profile (R^2 approximately 0.98), the worst for the wind speed (R^2 approximately 0.8). Wind component across the axis (v) is better captured by the model than along the axis (u). Surprisingly much large differences are observed between different PBL schemes for the mixing ratio. The best correlation is achieved using QNSE ($R^2=0.88$), the worst correlation for ACM2 ($R^2=0.75$). In general the

vertical profile evaluation shows the same weakness that is found for the surface relative humidity – WRF underestimate the mixing ratio.

Table 5. Model PBL scheme evaluation metrics for air temperature and relative humidity, in cases with strong wind (Cases 6, 7, 8 and 9) at Borisova gradina, Nadezhda, Pavlovo, Druzhba and Krasno selo (number of measurements - 480).

	<i>Mean</i>	<i>SD</i>	<i>MB</i>	<i>MAE</i>	<i>RMSE</i>	<i>R</i>
Temperature [°C]						
Observations	7.4	1.6				
QNSE	8.2	1.8	0.3	1.6	1.9	0.68
YSU	11.8	2.0	-0.1	1.9	2.2	0.69
BouLac	9.2	1.4	1.2	1.6	1.8	0.73
ACM2	8.6	1.7	0.7	1.6	1.8	0.69
Relative Humidity [%]						
Observations	75.2	9.1				
QNSE	75.9	9.1	-2.4	10.2	11.9	0.67
YSU	71.0	8.5	-3.7	9.2	10.4	0.71
BouLac	70.9	7.6	-7.5	10.3	12.1	0.69
ACM2	73.4	9.3	-4.4	10.4	11.7	0.71

Table 6. Model PBL scheme evaluation metrics for air temperature and relative humidity for 8 cases (from case 2 to 9), at SYNOP stations Dragoman and Sofia (number of measurements - 480).

	<i>Mean</i>	<i>St. Dev</i>	<i>MB</i>	<i>MAE</i>	<i>RMSE</i>	<i>R</i>
Temperature [°C]						
Observations	9.3	2.0				
QNSE	9.2	2.3	-0.1	1.6	1.9	0.80
YSU	9.6	2.0	0.3	1.2	1.4	0.82
BouLac	10.1	1.9	0.8	1.3	1.5	0.83
ACM2	9.9	2.3	0.2	1.4	1.7	0.82
Relative Humidity [%]						
Observations	71.1	10.0				
QNSE	71.2	10.6	0.1	11.2	13.2	0.58
YSU	68.5	8.9	-2.6	9.3	10.4	0.64
BouLac	66.3	7.9	-4.8	9.8	11.7	0.62
ACM2	68.9	9.6	-2.2	10.1	11.7	0.62

A number of studies on PBL sensitivity tests (Zhang & Zhang, 2004; Cheng and Steenburgh, 2005; de Meij et al., 2009; Gilliam & Pleim, 2010; Mass and Ovens, 2011; Jiménez and Dudhia, 2013; Gómez-Navarro et al., 2015; Dimitrova et al., 2016) are published for diverse domains and various combinations of model's options. Despite of all these efforts it is hard to select the best and universal PBL scheme as performance of different schemes is highly influenced by large variety of local conditions.

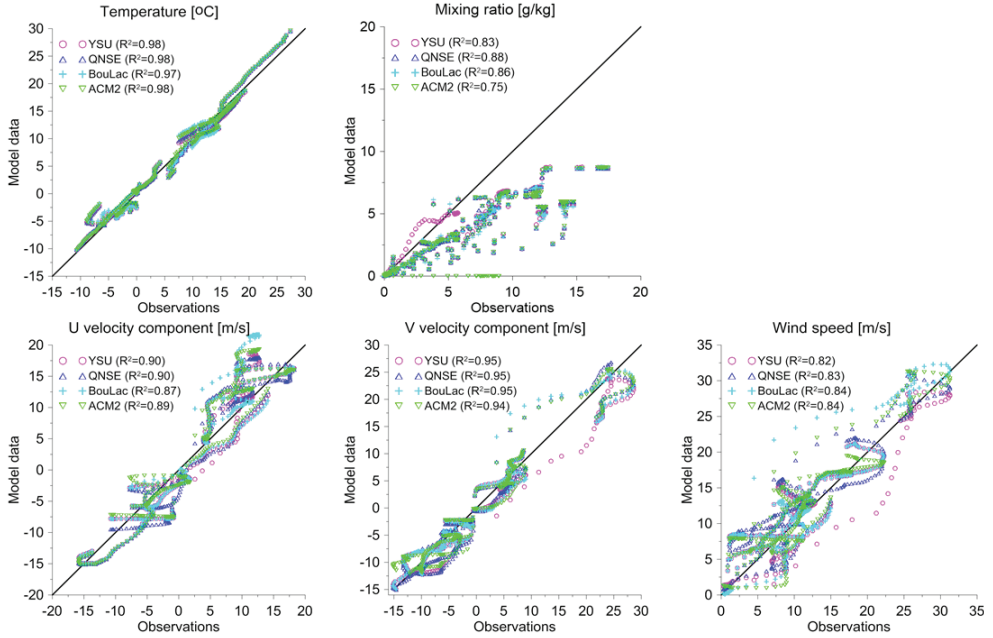


Fig. 2. Scatter plot of the vertical profiles of temperature, mixing ratio, wind speed and u and v wind components.

The choice of microphysics schemes highly affects the model's results for precipitation (Queen and Zhang, 2008), since microphysics includes explicitly resolved water vapor, cloud, and precipitation processes. Comparisons between different microphysics schemes are made for severe rainfall events (ElTahan M. and Magooda M., 2017) or different meteorological condition during summer and winter months (Borge et. al., 2008).

Several studies are carried out for the Sofia region during the recent years covering different aspects. Kirova & Batchvarova (2013) estimate the model abilities to perform convective conditions with one specific configuration using radiosonde profiles for 5 days on every 2 hours. Penchev & Peneva (2013) validate WRF model for icing conditions for one day and demonstrate very good correlation coefficient between the model and sounding data ($r = 0.91$ for the temperature and $r = 0.7-0.8$ for humidity). The YSU PBL and Double-Moment 6 class schemes are used in this study and the

results are similar to outcomes found here. The authors however show that for the wind the correlation is not so good especially in the low atmospheric layers. Manafov I. (2017) focus on improving the model performance for fog conditions at the Sofia airport comparing five PBL schemes for 18 cases and 6 microphysics schemes for 2 cases. The author found that QNSE is the best performing PBL scheme (one of the best in our study also) and Thompson for microphysics (Lin scheme is the best in our study). Test with various land surface models are performed in Manafov I. (2017) and Georgieva I. (2017), showing contradictory results regarding Noah LSM, which is used in this study.

3.2. Meso-scale circulation under different large-scale conditions

As already has been mentioned above, the purpose of this study is to model the specifics of the meso-scale circulation under different large-scale conditions for the Sofia region. All numerical results have been analyzed qualitatively by looking at the flow field plotted at 10 m and at 700 hPa level (undisturbed synoptic flow), and at the vertical cross sections along and across the valley axis. One example for the cases with strong wind (>10 m/s) is shown in Figs. 3 (cases 8 and 9) and 4 (cases 6 and 7). The Northwesterly synoptic current is slightly changed, and flows along the valley floor. Modification of the stream is significant mainly around the Vitosha Mountain. Tunnel effects following the gorges between Vitosha and surrounding mountains, stagnation at the windward and acceleration of the flow on the leeward slope are easily discernible.

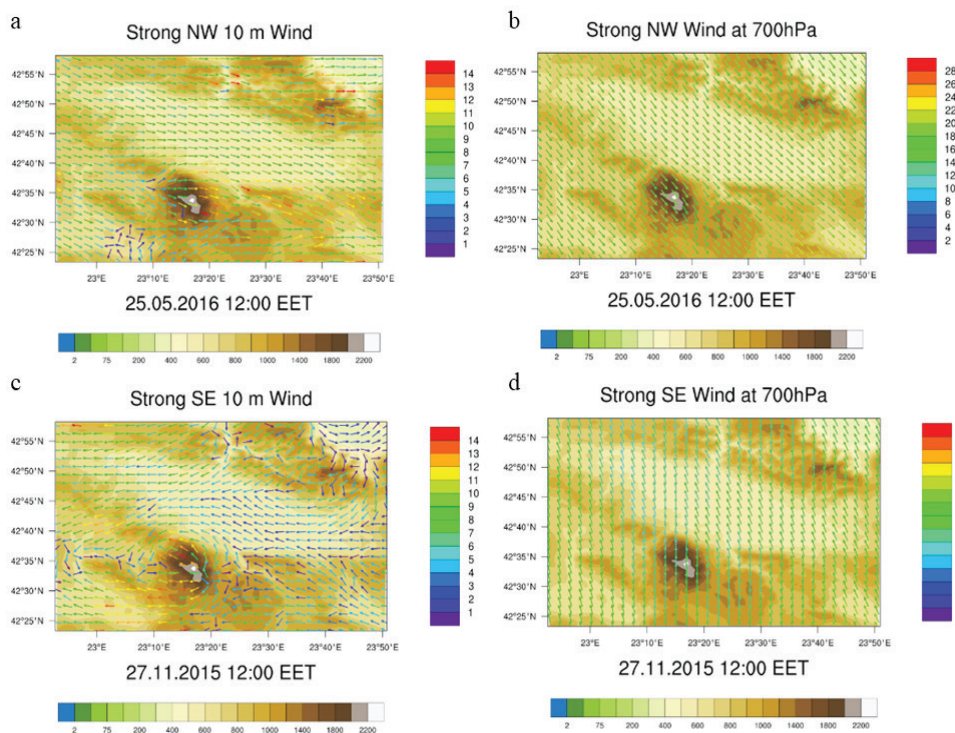


Fig. 3. Modification of the surface wind in Sofia valley (a, c) during synoptic flows along the valley axes – case 8 of northwesterly (b) and case 9 of southeasterly winds (d). The color bar (right) indicates weed speed in m/s; the bar (below) the model terrain height in meters.

This is the most common invasion for the Sofia valley (Blaskova et. al., 1983). The Southeasterly large scale flow is variable in the domain changing to Southern flow above the Vitosha Mountain. The collision with the obstacle makes the near surface flow pattern more complicated. The wind speed is significantly reduced inside the valley and the flow turns around the Vitosha Mountain forming lee vortex and stagnation region west of the obstacle. The observed flow pattern is in agreement with the laboratory experiment (Tucker, 1989).

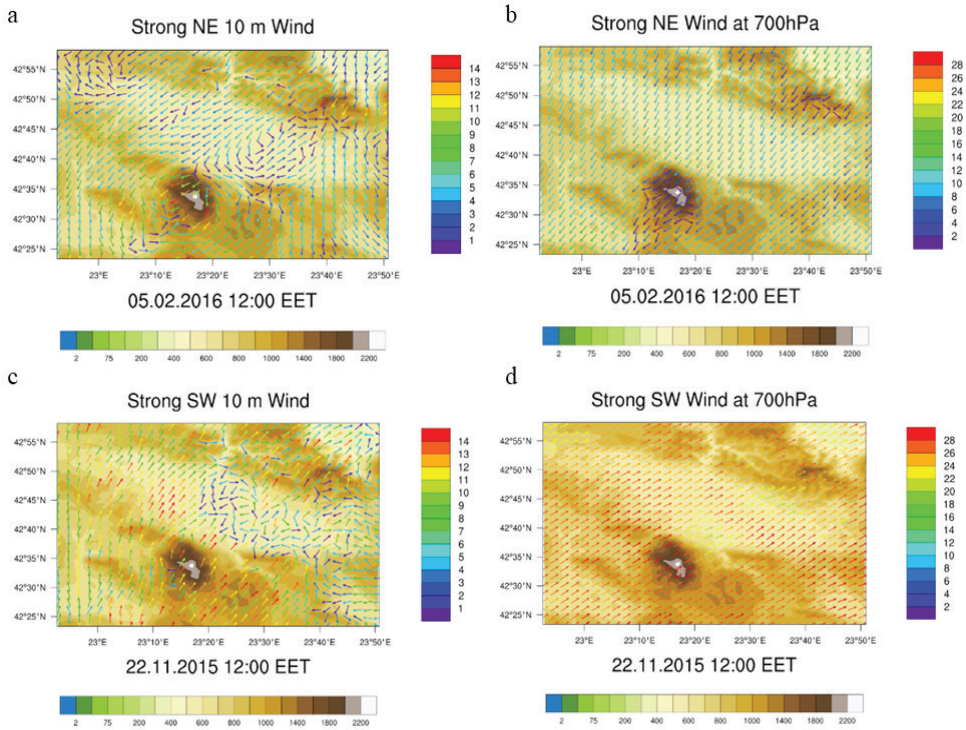


Fig. 4. Modification of the surface wind in Sofia valley during synoptic flows across the valley axes - Northeasterly flow and Southwesterly flow. The color bar (right) indicates weed speed in m/s; the bar (below) the model terrain height in meters.

More interesting is modification of the synoptic airflow when the direction is perpendicular to the main obstacles Stara Planina and Vitosha mountains. The Northeasterly synoptic flow collide with the Vitosha Mountain, some of the air is blocked, part of the flow splits around the obstacle forming stagnant area within the wake behind the mountain. Another part of the flow overturns against the main current, forming large vortex in the eastern part of the valley. The Southwesterly synoptic flow is the case with the highest wind speed more than 25 m/s at 700 hPa. The current has enough energy to overcome the Vitosha Mountain making large stagnation area in the wake behind the obstacle with weak return flow.

Vertical slides of the interpolated horizontal wind vectors over the chosen cross-section across the valley axis are shown for both interesting cases (cases 6 and 7), which

have been described in Fig. 4, and for the case with calm conditions. Fig. 5 corresponds to case 7 with strong Northeasterly synoptic wind (see fig. 4a, b), which hit the Vitosha Mountain. Three layers, with reverse flow in the middle, are simulated during the stable nocturnal conditions (fig. 5a, b).

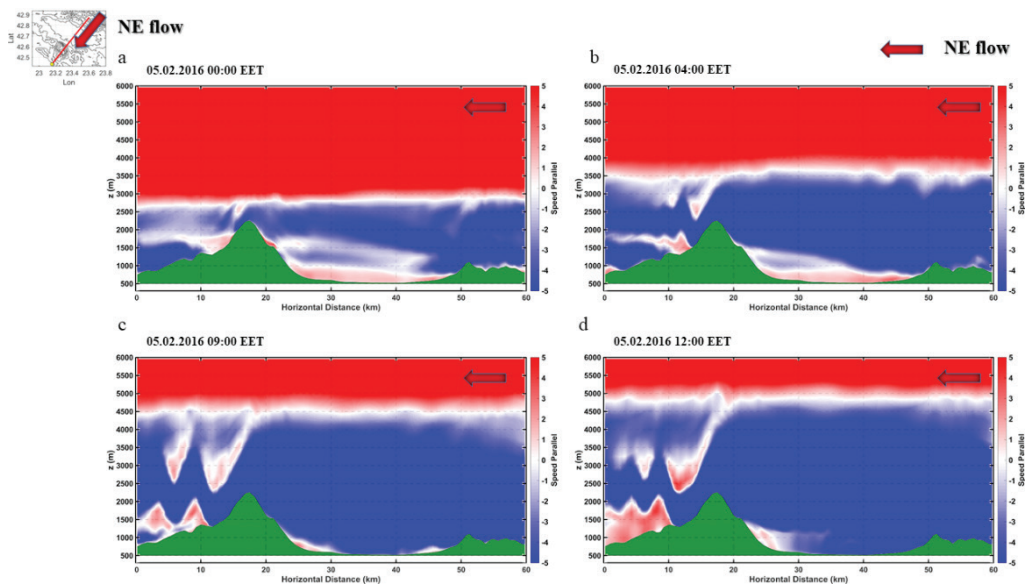


Fig. 5. Vertical slides of wind over the chosen cross-section (shown at the left upper corner) for YSU PBL scheme for the Case 7 - strong NE flow at different times.

The reversal flow depth increases with time and strong wind shear produces flow propagation behind the obstacle and large vortexes formation on the leeward slop of the Vitosha Mountain. Secondary return flow is observed inside the valley close to the ground. The disturbances grow with time forming lee-waves with maximum in amplitude before the sunrise (fig. 5c). After the sun rise the stable nocturnal layer becomes weaker, the magnitude of the lee-waves decreases, and they disappear at 12 EET (fig. 5d).

Fig. 6 corresponds to case 6 with very strong Southeasterly synoptic wind with speed more than 25 m/s (see fig. 4c, d). The airflow has enough energy to pass over the mountain forming patchy regions with reverse flow inside the wake of the obstacle. The disturbance mostly due to increase in roughness above the urban area leading to development of very complicated layered structure during the stable night conditions.

The slop flow formation can be observed in presence of weak synoptic flow – Case1 (fig. 7). During the night due to surface cooling thin layer colder than environment run downslope forming a downslope flow (fig. 7a) which strengthen with the increase in stability (fig. 7b). After the sun raise the ground heating reverse the process and after the morning transition (fig. 7c) well displayed anabatic flow inside the valley can be seen (fig. 7d).

*Numerical study of meso-scale circulation specifics in the Sofia region
under different large-scale conditions*

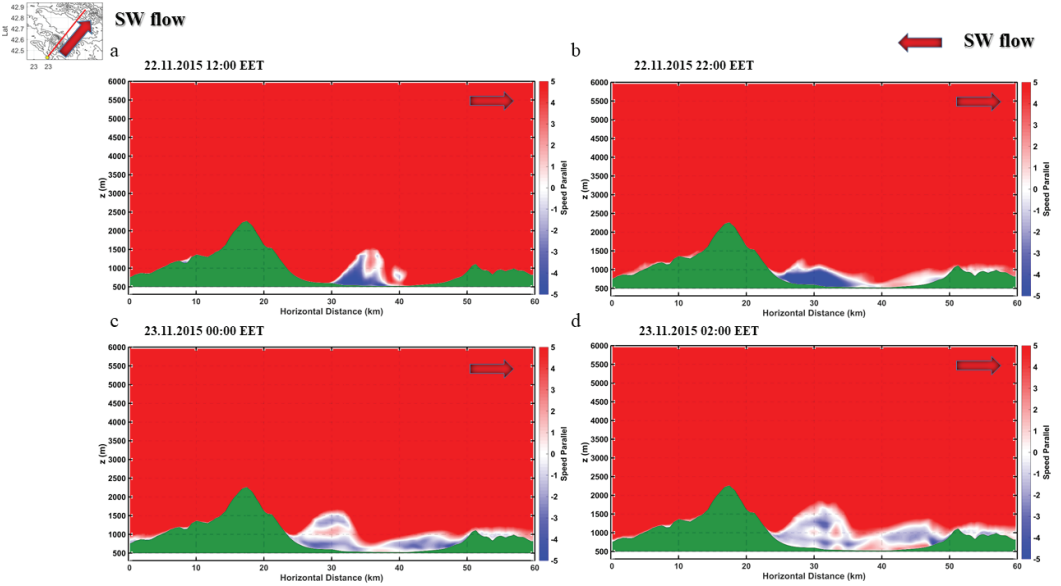


Fig. 6. Vertical slides of wind over the chosen cross-section (shown at the left upper corner) for YSU PBL scheme for Case 6 - strong SW flow at different times.

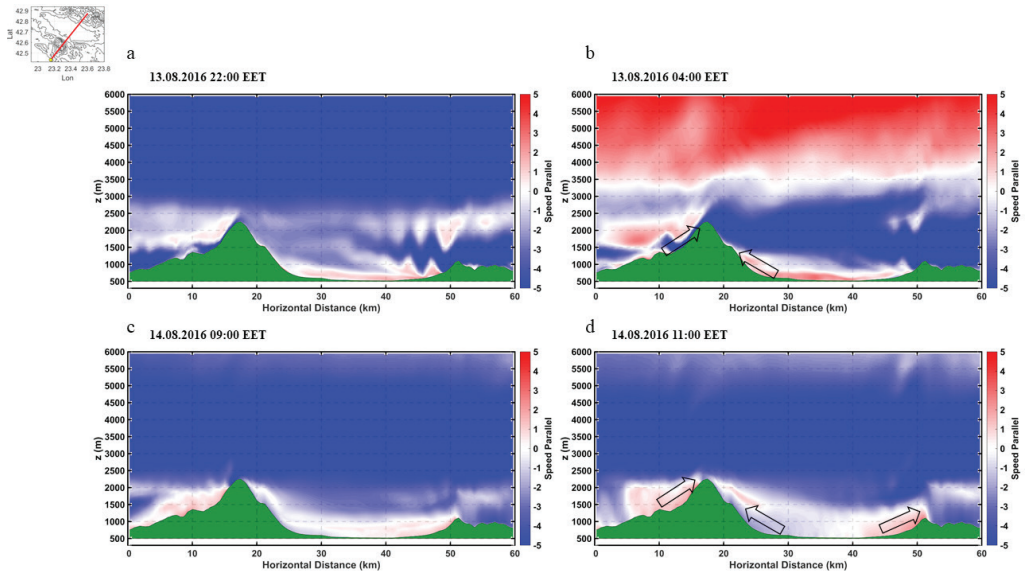


Fig. 7. Vertical slides of wind over the chosen cross-section (shown at the left upper corner) for YSU PBL scheme for Case 1 - calm conditions at different times.

5. CONCLUSIONS

Different PBL and microphysics schemes available in WRF model are evaluated in this study. Experimental data from 2 surface SYNOP sites, 6 automatic stations and daily radiosounding (at 12 UTC) are used to assess the model performance. Simple statistics for surface parameters (only temperature and relative humidity) and vertical profiles of temperature, mixing ratio and wind, show good model ability to describe the study cases. The model shows better agreement for the cases with moderate wind (cases 2, 3, 4 and 5) conditions in comparison to the strong synoptic winds (cases 6, 7, 8 and 9). The agreement between model data and observations is very good for the temperature and moderate for the wind speed and relative humidity. Two experiments have been conducted to estimate the best model performance using various schemes for microphysics and PBL with constant other options. Overall the Lin et al. scheme shows the best performance and it has been selected to be used for the PBL experiment. None of the PBL schemes is found to be superior, but all provide reasonable results. There is no significant difference in the horizontal flow pattern, but the main variations between different PBL schemes appears in the vertical wind speed profiles, with some cases of large over or underestimation of the observed values.

The modification of the synoptic flow within PBL due to the complex orography in Sofia region is substantial and Vitosha Mountain plays a significant role in this process. The large-scale flow remains unaffected above 700 hPa. Different mesoscale phenomena are captured with numerical simulations such as mountain lee waves, vortex shedding, stagnant area within the wake behind the obstacle, and nocturnal jet formation. Due to the downslope flows with different density coming from the surrounding mountains during nocturnal stable conditions several layers appear inside the valley. The diurnal evaluation of well mixed convective layer during the day and decrease of the PBL height during the night within the valley is also captured well by the model.

WRF model shows good performance and it is a very useful tool to study flow structure and variability. All of the meso-scale phenomena play significant role on the local PBL structure and microclimate. Due to the complex orography and the presence of huge urban area inside the valley it is difficult to separate the influence of different factors. Further investigation is needed to increase and analyse the number of events (days) inside the defined large scale conditions in order to get statistically significant representativeness of the specific meso-scale circulation in the Sofia valley.

ACKNOWLEDGEMENTS

This research is developed within the scope of the project DN4/7 (Study of the PBL structure and dynamics over complex terrain and urban area), funded by Research Fund at the Bulgarian Ministry of Education and Science.

REFERENCES

- Baines, P. G. and P. C. Manins, (1988), The principles of laboratory modelling of atmospheric flow over complex terrain. Manuscript. CSIRO Division of Atmospheric Research, Mordialloc, 3195, Australia.
- Blaskova D., L. Zlatkova, S. Lingova, Zh. Modeva, L. Subev, M. Teneva (1983), Climate and microclimate of Sofia. BAS, Sofia. (in Bulgarian).
- Borge, R., V. Alexandrov, J. del Vas, J. Lumbreras, and E. Rodríguez, (2008), A comprehensive sensitivity analysis of the WRF model for air quality applications over the Iberian Peninsula, *Atmos. Environ.*, 42, 8560–8574.
- Bornstein, R. F., D. R. Leone, D. J. Galley, (1987), The generalizability of subliminal mere exposure effects: Influence of stimuli perceived without awareness on social behaviour. *Journal of Personality and Social Psychology*, 53, 1070-1079.
- Bougeault, P., P. Lacarrere, (1989), Parametrization of orography-induced turbulence in a mesobeta-scale model. *Mon Weather Rev* 117(8):1872–1890.
- Bretherton, S. Christopher and Sungsu Park, (2009), A new moist turbulence parameterization in the Community Atmosphere Model. *J. Climate*, 22, 3422–3448.
- Chen, F., and J. Dudhia, (2001), Coupling an advanced land surface-hydrology model with the Penn State-NCAR MM5 modelling system. Part I: Model implementation and sensitivity. *Mon Weather Rev* 129:569–585.
- Cheng, W. Y. Y. and Steenburgh, W. J., (2005), Evaluation of Surface Sensible Weather Forecasts by the WRF and the Eta Models over the Western United States, *Weather Forecast.*, 20, 812–821, doi:10.1175/WAF885.1.
- De Meij, A., A. Gizella, C. Cuvelier, P. Thunis, B. Bessagnet, J. F. Vinuesa, L. Minut, and H. M. Kelder, (2009), The impact of MM5 and WRF meteorology over complex terrain on CHIMERE model calculations, *Atmos. Chem. Phys.*, 9, 6611–6632.
- Dimitrova R., Silver Z., Zsedrovits T., Hocut C., Leo L. S., Di Sabatino S., Fernando H. J. S., (2016), Assessment of Planetary Boundary-Layer Schemes in the Weather Research and Forecasting Mesoscale Model Using MATERHORN Field Data, *Boundary-Layer Meteorol*, 159, 589–609, doi 10.1007/s10546-015-0095-8.
- Dixit, P. N., and D. Chen, (2011), Effect of topography on farm-scale spatial variation in extreme temperatures in the Southern Mallee of Victoria, Australia. *Theor. Appl. Climatol.*, 103, 533-542.
- Dudhia, J., (1989), Numerical study of convection observed during the winter monsoon experiment using a mesoscale two-dimensional model. *J Atmos Sci* 46:3077–3107.
- ElTahan, M. and M. Magooda, 2017, Evaluation of different WRF microphysics schemes: severe rainfall over Egypt case study, *Physics - Atmospheric and Oceanic Physics*.
- Emmanuel, R. & H. J. S. Fernando, (2007), Urban heat islands and arid climates: role of urban form and thermal properties in Colombo, Sri Lanka and Phoenix, USA, *Climate Research* 34 (3), 241.
- Gilliam, R., and J. Pleim, (2010), Performance assessment of the Pleim-Xiu LSM, Pleim surface-layer and ACM PBL Physics in version 3.0 of WRF-ARW (accepted by *Journal of Applied Meteorology and Climate*).
- Gómez-Navarro, J. J., Raible, C., C. and Dierer S., Sensitivity of the WRF model to PBL parametrisations and nesting techniques: evaluation of wind storms over complex terrain, *Geosci. Model Dev.*, 8, 3349–3363, 2015.

- Georgieva, I., (2017), Local transport and chemical transformations in the atmosphere, PhD thesis, (in Bulgarian).
- Grell, G. A. and D. Devenyi, (2002), A generalized approach to parameterizing convection combining ensemble and data assimilation techniques. *Geophys. Res. Lett.* 29(1693).
- Hong, S., Y. Noh, J. Dudhia, (2006), A new vertical diffusion package with an explicit treatment of entrainment processes. *Mon Weather Rev* 134(9):2318–2341.
- Hong, S. Y. and J. O. J. Lim, (2006), The WRF single-moment 6-class microphysics scheme (WSM6). *J. Korean Meteor. Soc.*, 42, 129–151.
- Hunt, J. C. R., M. Maslin, T. Killean, P. Backlund, J. Schellnhuber, (2007), Introduction: Climate change and urban areas; Research dialog in a policy framework. *Phil. Trans. Roy. Soc. (London)* DOI: 10.1098/ersta.1007.2089.
- Jiménez, P. A. and Dudhia, J., Improving the Representation of Resolved and Unresolved Topographic Effects on Surface Wind in the WRF Model, *J. Appl. Meteorol. Clim.*, 51, 300–316, doi:10.1175/JAMC-D-11-084.1, 2012.
- Jiménez, P. A. and Dudhia, J., (2013), On the Ability of the WRF Model to Reproduce the Surface Wind Direction over Complex Terrain, *J. Appl. Meteorol. Clim.*, 52, 1610–1617, doi:10.1175/JAMC-D-12-0266.1.
- Kirova H. and E. Batchvarova, (2013), Verification of meso-meteorological model using aerological data from the Sofia experiment 2003, Proceedings of the 2nd National Congress in Physical Sciences, 25- 29 September 2013, Sofia, Bulgaria (in Bulgarian).
- Lin, Y. L., R. D. Farley, H. D. Orville, (1983), Bulk parametrization of the snow field in a cloud model. *J Appl Meteorol* 22:1065–1092.
- Manafov, I., (2017), Fog forecast for Sofia airport, PhD thesis, (in Bulgarian).
- Mass, C. and Ovens, D., (2011), Fixing WRF's high speed wind bias: A new subgrid scale drag parameterization and the role of detailed verification, in: 24th Conf. on Weather and Forecasting/20th Conf. on Numerical Weather Prediction, Vol. 9B.6, available at: <http://ams.confex.com/ams/91Annual/webprogram/Paper180011.html> (last access: 21 October 2015), *Amer. Meteor. Soc.*
- Mlawer, E. J., S. J. Taubman, P. D. Brown, M. J. Iacono, S. A. Clough, (1997), Radiative transfer for inhomogeneous atmospheres: RRTM, a validated correlated-k model for the longwave. *J Geophys Res Atmos* 102(14):16,663–16,682.
- Oke, T. R., (1988), Street design and urban canopy layer climate. *Energy and Buildings*, 11, 103–113.
- Penchev R. and E. Peneva, (2013), Numerical simulation of extreme convective events during 2012 in Bulgaria using the weather forecast model WRF, Proceedings of the 2nd National Congress in Physical Sciences, 25-29 September 2013, Sofia, Bulgaria (in Bulgarian).
- Pielke, R. A., (2013), *Mesoscale Meteorological Modelling*, Academic Press is an imprint of Elsevier, Third Edition, p. 716.
- Pleim, J. E., (2007), A combined local and nonlocal closure model for the atmospheric boundary layer. Part I: Model description and testing. *J Appl Meteorol Clim* 46(9):1383–1395 .
- Queen, A.N., Zhang, Y, 2008. Examining the sensitivity of MM5-CMAQ predictions to explicit microphysics schemes and horizontal grid resolutions. Part II - PM concentration and wet deposition predictions. *Atmospheric Environment*. doi:10.1016/j.atmosenv.2007.12.066.
- Snyder, W. H. and Coauthors, (1985), The structure of strongly stratified flow over hills: dividing-740 streamline concept. *J. Fluid Mech.*, 152, 249-288.

- Sukoriansky, S., B. Galperin, V. Perov, (2005), Application of a new spectral theory of stably stratified turbulence to the atmospheric boundary layer over sea ice. *Boundary-Layer Meteorol* 117(2):231–257.
- Tao, Wei-Kuo, J. Simpson, M. McCumber, (1989), An Ice–Water Saturation Adjustment. *Mon. Wea. Rev.*, 117, 231–235.
- Thompson, G., P. R. Field, R. M. Rasmussen, W. D. Hall, (2008), Explicit Forecasts of Winter Precipitation Using an Improved Bulk Microphysics Scheme. Part II: Implementation of a New Snow Parameterization. *Mon. Wea. Rev.*, 136, 5095–5115.
- Tucker, G. B., (1989), Laboratory modelling of air flow in the Sofia valley Bulg. *Geophys. J.* 15, 92-100, [pp. 450, 453].
- Vladimirov, E., R. Dimitrova and V. Danchevski, Sensitivity of the WRF model results to topography and land cover: study for the Sofia region, *Annuaire de l'Université de Sofia "St. Kliment Ohridski"*, Faculté de Physique - accepted for publication.
- Zardi, D. and C. D. Whiteman, (2012), *Mountain weather research and forecasting*, Chapter 2, p. 74.
- Zhang, D.-L., and W.-Z. Zhang, 2004. Diurnal cycles of surface winds and temperatures as simulated by five boundary layer parameterizations, *J. App. Meteor.*, 114, 157–169.